

# Selective Synthesis and Characterization of Single-Crystal Silver Molybdate/Tungstate Nanowires by a Hydrothermal Process

Xianjin Cui,<sup>[a, b]</sup> Shu-Hong Yu,<sup>\*[a, b]</sup> Lingling Li,<sup>[c]</sup> Liu Biao,<sup>[b]</sup> Huabin Li,<sup>[b]</sup> Maosong Mo,<sup>[d]</sup> and Xian-Ming Liu<sup>[a]</sup>

**Abstract:** Selective synthesis of uniform single crystalline silver molybdate/tungstate nanorods/nanowires in large scale can be easily realized by a facile hydrothermal recrystallization technique. The synthesis is strongly dependent on the pH conditions, temperature, and reaction time. The phase transformation was examined in details. Pure  $\text{Ag}_2\text{MoO}_4$  and  $\text{Ag}_6\text{Mo}_{10}\text{O}_{33}$  can be easily obtained under neutral condition

and pH 2, respectively, whereas other mixed phases of  $\text{Mo}_{17}\text{O}_{47}$ ,  $\text{Ag}_2\text{Mo}_2\text{O}_7$ ,  $\text{Ag}_6\text{Mo}_{10}\text{O}_{33}$  were observed under different pH conditions.  $\text{Ag}_6\text{Mo}_{10}\text{O}_{33}$  nanowires with uniform diameter 50–60 nm and length up to several hun-

**Keywords:** crystallization · molybdates · nanorods · nanowires · single crystals · tungsten

dred micrometers were synthesized in large scale for the first time at 140 °C. The melting point of  $\text{Ag}_6\text{Mo}_{10}\text{O}_{33}$  nanowires were found to be about 238 °C. Similarly,  $\text{Ag}_2\text{WO}_4$ , and  $\text{Ag}_2\text{W}_2\text{O}_7$  nanorods/nanowires can be selectively synthesized by controlling pH value. The results demonstrated that this route could be a potential mild way to selectively synthesize various molybdate nanowires with various phases in large scale.

## Introduction

Searching for new strategies toward one dimensional nano-sized building blocks such as nanorods, nanowires, nanotubes, and nanobelts has attracted intensive interest because of their distinctive geometries, novel physical and chemical properties, and potential applications in nanodevices.<sup>[1,2]</sup> These systems are expected to display the size and shape dependent optical, magnetic, and electronic properties.<sup>[3–6]</sup>

Exploration of new synthetic routes for preparing novel nanocrystals with structural speciality and complexity has

been a recent focus.<sup>[7]</sup> The main synthesis techniques for dimensional (1D) nanostructures include template directed growth methods such as carbon nanotubes,<sup>[8]</sup> porous aluminum template,<sup>[9]</sup> vapor–liquid–solid (VLS) mechanism,<sup>[10]</sup> and vapor–solid (VS) mechanism.<sup>[11]</sup> In contrast, the solution approaches have been proved to provide an alternative route for the synthesis of 1D nanostructures.<sup>[5,12–17]</sup> Especially, hydrothermal process has been successfully applied for the synthesis of low dimensional nanorods/nanowires/nanotubes.<sup>[7b,18–20]</sup>

Recently, the synthesis of low dimensional metal molybdates and tungstates materials such as  $\text{BaWO}_4$  nanorods,<sup>[14d]</sup>  $\text{CdWO}_4$  nanorods,<sup>[15,21]</sup>  $\text{MoO}_3$  nanorods<sup>[22]</sup> have attracted a lot of recent interests due to their strong application potential in various fields<sup>[23]</sup> such as photoluminescence,<sup>[24]</sup> microwave applications,<sup>[25]</sup> optical fibers,<sup>[26]</sup> scintillator materials,<sup>[27]</sup> humidity sensor,<sup>[28]</sup> magnetic properties,<sup>[29]</sup> and catalyst.<sup>[30]</sup> Most previous approaches for preparation of these families of molybdates and tungstates need high temperature and hard reaction conditions such as the solid state metathesis reaction at 1000 °C,<sup>[31]</sup> and sol–gel method.<sup>[32]</sup> Few reports are related with the synthesis of metal molybdates through solution methods.<sup>[33]</sup> Silver tungstates such as  $\text{Ag}_2\text{Mo}_4\text{O}_{13}$ ,  $\text{Ag}_2\text{Mo}_2\text{O}_7$ , and  $\text{Ag}_2\text{MoO}_4$  were traditionally synthesized by straight and harsh reaction in  $\text{MoO}_3/\text{Ag}_2\text{O}$  system.<sup>[34]</sup> These materials have high electrical conductivity and usually have found important applications in conducting glass.<sup>[35]</sup> However, solution synthesis of silver molybdates nanorods/nanowires was not found in literature up till now.

[a] Mr. X. Cui, Prof. Dr. S.-H. Yu, X.-M. Liu  
Structure Research Laboratory of CAS  
University of Science and Technology of China  
Hefei 230026 (P.R. China)  
Fax: (+86) 551-360-3040  
E-mail: shyu@ustc.edu.cn

[b] Mr. X. Cui, Prof. Dr. S.-H. Yu, L. Biao, H. Li  
Department of Materials Science and Engineering  
University of Science and Technology of China  
Hefei 230026 (P.R. China)  
Fax: (+86) 551-360-040  
E-mail: shyu@ustc.edu.cn

[c] L. Li  
Department of Polymer Science and Engineering  
University of Science and Technology of China  
Hefei 230026 (P.R. China)

[d] Dr. M. Mo  
Department of Chemistry  
University of Science and Technology of China  
Hefei 230026 (P.R. China)

Recently, our group has reported a general synthesis of tungstate nanorods/nanowires by hydrothermal method without using any ligand (or surfactant, or polymer).<sup>[36]</sup>

In this paper, we report how to selectively synthesize silver molybdate nanorods/nanowires in large scale through a simple hydrothermal approach. The influence of pH, reaction time, and temperature on the phase transformation was discussed. Increasing temperature leads to an increase in diameter of the nanowires.

## Results and Discussion

Hydrothermal treatment of an amorphous particulate dispersion made of  $\text{AgNO}_3$  and  $(\text{NH}_4)_6\text{Mo}_7\text{O}_{24}$  at  $140^\circ\text{C}$  for 12 h led to the formation of pure phase  $\text{Ag}_2\text{MoO}_4$  with well crystallinity as shown in Figure 1a, all reflection peaks of the different product prepared at pH 7 can be easily indexed as a pure cubic structure with cell parameters  $a = 9.26 \text{ \AA}$ , which is in good agreement with the previous literature (JCPDS Card number: 76-1747). TEM image shows that the product was composed of irregular particles with average size of 1–2  $\mu\text{m}$ .

However, when the more acidic solution was used, different phases were obtained as shown in Figures 1 and 2 and Table 1. A mixture of anorthic  $\text{Ag}_6\text{Mo}_{10}\text{O}_{33}$  (JCPDS Card: 72-1689,  $a = 7.59$ ,  $b = 8.31$ ,  $c = 11.42 \text{ \AA}$ ,  $\alpha = 82.6$ ,  $\beta = 102.9$ ,  $\gamma = 106.4^\circ$ ) and anorthic  $\text{Ag}_2\text{Mo}_2\text{O}_7$  (JCPDS Card: 75-1505,  $a = 6.095$ ,  $b = 7.501$ ,  $c = 7.681 \text{ \AA}$ ,  $\alpha = 110.4$ ,  $\beta = 93.3$ ,  $\gamma = 13.5^\circ$ ) was obtained at pH 5 as detected by the X-ray diffraction pattern (Figure 1b).

The phases such as  $\text{Ag}_6\text{Mo}_{10}\text{O}_{33}$ ,  $\text{Ag}_2\text{Mo}_2\text{O}_7$ , and  $\text{Mo}_{17}\text{O}_{47}$  were observed in the samples obtained at different pH value. With pH decreasing from 5 to 3, the products were found to be a mixture of  $\text{Ag}_6\text{Mo}_{10}\text{O}_{33}$  and  $\text{Ag}_2\text{Mo}_2\text{O}_7$ , and the content of  $\text{Ag}_6\text{Mo}_{10}\text{O}_{33}$  phase increased. Pure  $\text{Ag}_6\text{Mo}_{10}\text{O}_{33}$  phase can be obtained at pH 2 as shown in Figure 2a. TEM image (Figure 3a) and SEM image (Figure 4b)

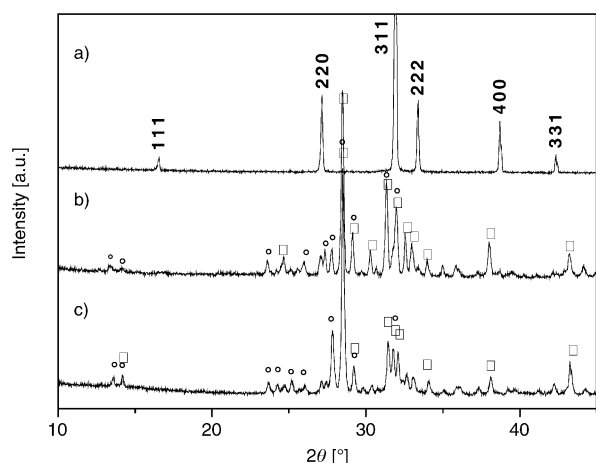


Figure 1. XRD patterns of the products obtained at different pH,  $140^\circ\text{C}$ , 12 h. a) pH 7,  $[\text{AgNO}_3] = 0.1 \text{ M}$ ,  $[(\text{NH}_4)_6\text{Mo}_7\text{O}_{24}] = 0.014 \text{ M}$ . b) pH 5,  $[\text{AgNO}_3] = 0.05 \text{ M}$ ,  $[(\text{NH}_4)_6\text{Mo}_7\text{O}_{24}] = 0.014 \text{ M}$ . c) pH 4,  $[\text{AgNO}_3] = 0.05 \text{ M}$ ,  $[(\text{NH}_4)_6\text{Mo}_7\text{O}_{24}] = 0.014 \text{ M}$ . □:  $\text{Ag}_2\text{Mo}_2\text{O}_7$ ; ○:  $\text{Ag}_6\text{Mo}_{10}\text{O}_{33}$ .

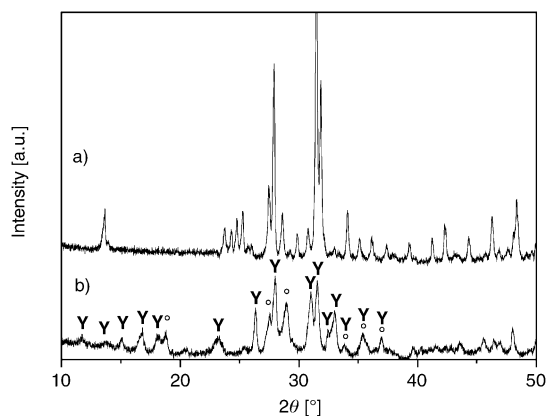


Figure 2. XRD patterns of the products obtained at different pH,  $[\text{AgNO}_3] = 0.05 \text{ M}$ ,  $[(\text{NH}_4)_6\text{Mo}_7\text{O}_{24}] = 0.014 \text{ M}$ ,  $140^\circ\text{C}$ , 12 h. a) pH 2. b) pH 1. ○:  $\text{Ag}_6\text{Mo}_{10}\text{O}_{33}$ , □:  $\text{Mo}_{17}\text{O}_{47}$ .

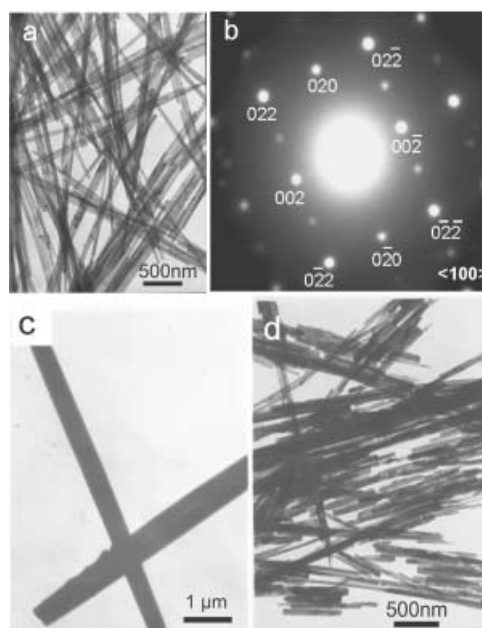


Figure 3. a), b) TEM image and electron diffraction pattern of  $\text{Ag}_6\text{Mo}_{10}\text{O}_{33}$  nanowires.  $[\text{AgNO}_3] = 0.1 \text{ M}$ ,  $[(\text{NH}_4)_6\text{Mo}_7\text{O}_{24}] = 0.014 \text{ M}$ , pH 2,  $140^\circ\text{C}$ , 12 h. a) TEM image; b) Electron diffraction pattern taken along [100] zone axis, showing that the nanowires are perfect single crystal. c) TEM image of a mixture containing  $\text{Ag}_6\text{Mo}_{10}\text{O}_{33}$  and  $\text{Ag}_2\text{Mo}_2\text{O}_7$ .  $[\text{AgNO}_3] = 0.1 \text{ M}$ ,  $[(\text{NH}_4)_6\text{Mo}_7\text{O}_{24}] = 0.014 \text{ M}$ , pH 3,  $140^\circ\text{C}$ , 12 h. d) TEM image of a mixture of two intermediate phases  $\text{Ag}_{1.028}\text{H}_{1.852}\text{Mo}_{5.52}\text{O}_{18}$  and  $\text{Ag}_2\text{Mo}_3\text{O}_{10}\cdot 8\text{H}_2\text{O}$ .  $[\text{AgNO}_3] = 0.1 \text{ M}$ ,  $[(\text{NH}_4)_6\text{Mo}_7\text{O}_{24}] = 0.014 \text{ M}$ , pH 2,  $140^\circ\text{C}$ , 6 h.

show that uniform nanowires with diameter of 50 nm and length up to several hundred micrometers. However, a small amount of large fiber bundles with diameter about 2–3  $\mu\text{m}$  can also be observed (Figure 4a). If the pH dropped to 3, the product was a mixture of  $\text{Ag}_6\text{Mo}_{10}\text{O}_{33}$  and  $\text{Ag}_2\text{Mo}_2\text{O}_7$  (Table 1). TEM image in Figure 3c shows that the particles are also rod-like and the diameter is about 500 nm.

When the pH value was further decreased to 1, a mixture of  $\text{Mo}_{17}\text{O}_{47}$  and  $\text{Ag}_6\text{Mo}_{10}\text{O}_{33}$  was detected as shown in Figure 2b. Interestingly, a mixture of two intermediate phases hexagonal  $\text{Ag}_{1.028}\text{H}_{1.852}\text{Mo}_{5.52}\text{O}_{18}$  (JCPDS Card: 83-1173) and

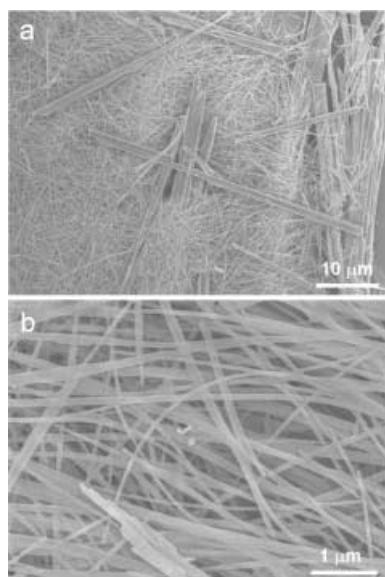


Figure 4. SEM images of the  $\text{Ag}_6\text{Mo}_{10}\text{O}_{33}$  nanowires obtained at pH 2,  $[\text{AgNO}_3]=0.1\text{ M}$ ,  $[(\text{NH}_4)_6\text{Mo}_7\text{O}_{24}]=0.014\text{ M}$ ,  $140^\circ\text{C}$ , 12 h: a) a general view shows the coexistence of the very uniform extremely long nanowires and small amount of large nanofiber bundles; b) a high resolution image shows extremely long nanowires.

$$\cos\phi = d_1d_2V^2 \cdot [S_{11}h_1h_2 + S_{22}k_1k_2 + S_{33}l_1l_2 + S_{23}(k_1l_2+k_2l_1) + S_{13}(l_1h_2+l_2h_1) + S_{12}(h_1k_2+h_2k_1)] \quad (1)$$

$$V = abc\sqrt{1 - \cos^2\alpha - \cos^2\beta - \cos^2\gamma + 2\cos\alpha\cos\beta\cos\gamma} \quad (2)$$

$$S_{11} = b^2c^2\sin^2\alpha; S_{22} = a^2c^2\sin^2\beta \quad (3)$$

$$S_{33} = a^2b^2\sin^2\gamma \quad (4)$$

$$S_{12} = abc^2(\cos\alpha\cos\beta - \cos\gamma) \quad (5)$$

$$S_{23} = a^2bc(\cos\beta\cos\gamma - \cos\alpha), S = ab^2c(\cos\alpha\cos\gamma - \cos\beta) \quad (6)$$

Table 1. The main phases obtained at different pH (\*: dominant phase).

pH	Phase	Shape	Diameter
1	$\text{Mo}_{17}\text{O}_{47}^* + \text{Ag}_6\text{Mo}_{10}\text{O}_{33}$	nanowires	30–50 nm
2	$\text{Ag}_6\text{Mo}_{10}\text{O}_{33}$	nanowires	50 nm
3	$\text{Ag}_6\text{Mo}_{10}\text{O}_{33}^* + \text{Ag}_2\text{Mo}_2\text{O}_7$	nanowires	50–60 nm
4	$\text{Ag}_6\text{Mo}_{10}\text{O}_{33} + \text{Ag}_2\text{Mo}_2\text{O}_7$	nanowires	50–60 nm
5	$\text{Ag}_6\text{Mo}_{10}\text{O}_{33} + \text{Ag}_2\text{Mo}_2\text{O}_7^*$	nanowires	50 nm
7	$\text{Ag}_2\text{MoO}_4$	irregular particles	1–2 μm

orthorhombic  $\text{Ag}_2\text{Mo}_3\text{O}_{10}\cdot 8\text{H}_2\text{O}$  (JCPDS Card: 39-0045) was observed when the reaction was conducted for 6 h (XRD data not shown). TEM image in Figure 3d shows that the product was also wire-like structures with diameter about 40 nm and an aspect ratio of 10–50. Very rough surface suggested that these nanorods could be not stable and may start to transform into other phases. Further prolonging the reaction time up to 12 h, the  $\text{Ag}_6\text{Mo}_{10}\text{O}_3$  nanowires formed. An increase in temperature leads to an increase in diameter of the nanowires.

High resolution TEM images in Figure 4 shows that very tiny nanoparticles with size of 5 nm attached on the backbone of the  $\text{Ag}_6\text{Mo}_{10}\text{O}_{33}$  nanowires. Interestingly, after exposed under TEM electron beams, a lot of tiny nanoparticles appeared on the backbone of the nanowires. We believe that the  $\text{Ag}_6\text{Mo}_{10}\text{O}_{33}$  nanowires are not stable under electron beam irradiation. After exposed for longer time, many tiny nanoparticles appeared on the wire surfaces and these particles tend to become amorphous as confirmed by electron diffraction observation. TG-DTA analysis shows that the melting point of this compound is about  $238^\circ\text{C}$ , suggesting that the nanowires could be destroyed under too longer electron beam irradiation. The detailed analysis of such phenomena is needed in future.

The lattice resolved HRTEM images were shown in Figure 5d and e. The lattice spacing  $3.16\text{ \AA}$  corresponding to (022) planes. The angle between (002) and (022) can be calculated from the following formulae for anorthic system:

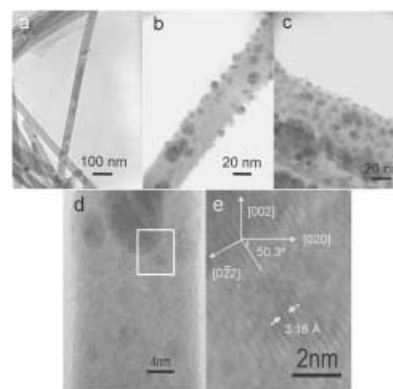


Figure 5. High magnification SEM images of the  $\text{Ag}_6\text{Mo}_{10}\text{O}_{33}$  nanowires obtained at pH 2,  $[\text{AgNO}_3]=0.1\text{ M}$ ,  $[(\text{NH}_4)_6\text{Mo}_7\text{O}_{24}]=0.014\text{ M}$ ,  $140^\circ\text{C}$ , 12 h: a) a general view shows there are very tiny nanoparticles on the surface of the nanowires; b)–c) high resolution image show the surface structures of the nanowires after exposed electron beams; d) lattice resolved HRTEM image, showing that the nanowires grow along [002], which also corresponds to that shown in its electron diffraction pattern in Figure 3b.

Where cell parameters for the anorthic  $\text{Ag}_6\text{Mo}_{10}\text{O}_{33}$  are  $a=7.59$ ,  $b=8.31$ ,  $c=11.42\text{ \AA}$ ,  $\alpha=82.6$ ,  $\beta=102.9$ ,  $\gamma=106.4^\circ$  (JCPDS Card: 72-1689). The calculated angle between (002) and (02) is  $50.3^\circ$ , which is consistent with that observed in Figure 5d. In addition, the angle between (020) and (022) is  $148.4^\circ$ , which fits the measured value very well too. These results suggested that the nanowires grow preferentially along  $c$  axis. (See also the electron diffraction pattern shown in Figure 3b).

Figure 6 shows the X-ray photoelectron spectroscopy (XPS) spectrum of  $\text{Ag}_6\text{Mo}_{10}\text{O}_{33}$  nanowires. The survey indicates the presence of  $\text{Mo}^{\text{VI}}$  and Ag as well as C from reference and O from absorbed  $\text{CO}_2$  molecules. Ag 3d spectrum (Figure 6b) is very similar to that measured for  $\text{Ag}^{\text{I}}$  in silver oxides ( $\text{Ag}_2\text{O}$ ).<sup>[37]</sup> The binding energy of  $\text{Mo } 3d_{5/2}$  in the  $\text{Ag}_6\text{Mo}_{10}\text{O}_{33}$  nanowires is identical with that of pure  $\alpha\text{-MoO}_3$  ( $232.6\text{ eV}$ ).<sup>[38]</sup> The core-level O 1s spectrum in Figure 6d

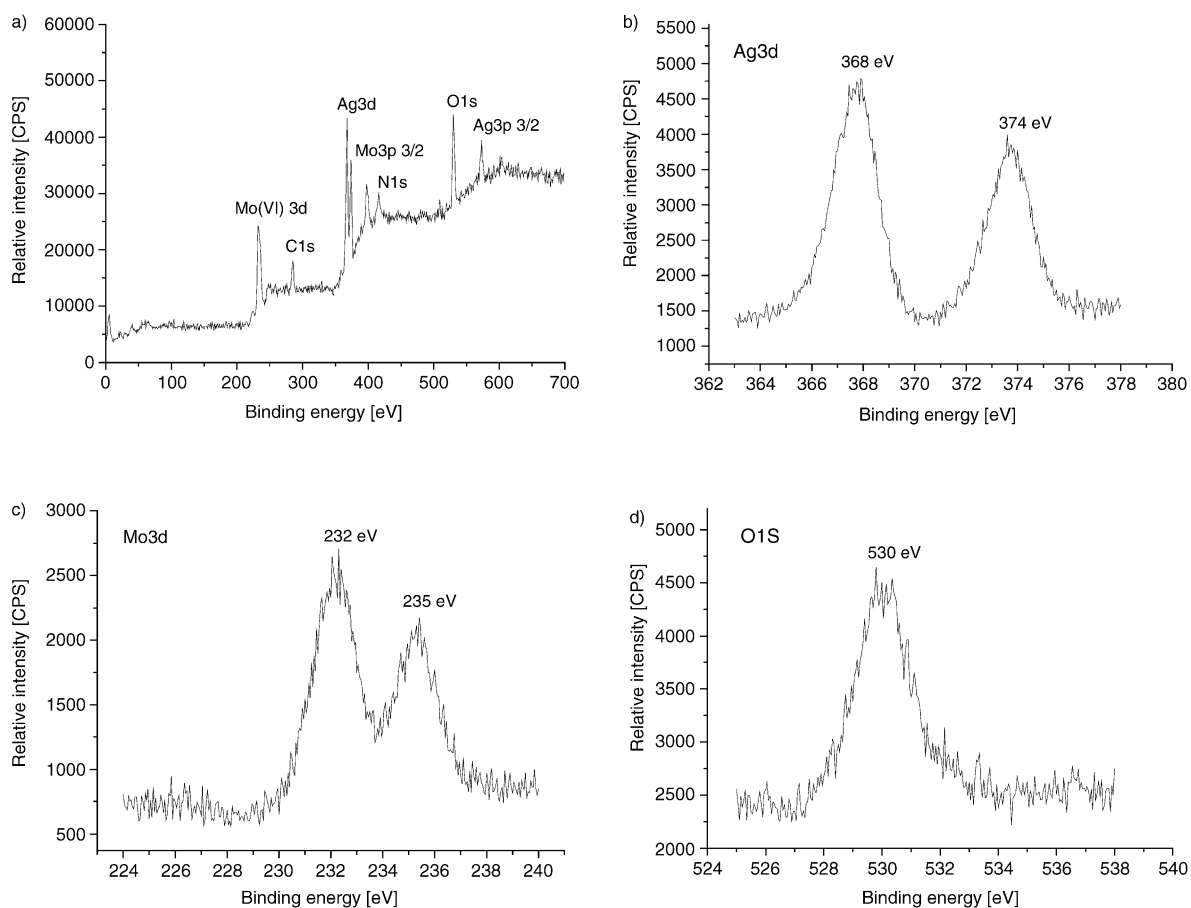


Figure 6. XPS spectrum of the  $\text{Ag}_6\text{Mo}_{10}\text{O}_{33}$  nanowires. The sample was obtained at pH 2.  $[\text{AgNO}_3]=0.1\text{ M}$ ,  $[(\text{NH}_4)_6\text{Mo}_7\text{O}_{24}]=0.014\text{ M}$ , pH 2,  $140^\circ\text{C}$ , 12 h. a) A full spectrum. b)  $\text{Ag}_{3d}$  core-level data. c)  $\text{Mo}_{3d}^{\text{VI}}$  core-level data. d)  $\text{O}_{1s}$  core-level data.

shown a peak at 530 eV, which is also similar to that in  $\text{CuO}$  or  $\text{Ag}_2\text{O}$  systems.<sup>[39]</sup>

Similarly, perfect single crystals of  $\alpha\text{-Ag}_2\text{WO}_4$  nanorods and  $\text{Ag}_2\text{W}_2\text{O}_7$  nanowires can be selectively synthesized at pH 9 and 2, respectively. The sample obtained at pH 9 can be indexed as orthorhombic  $\alpha\text{-Ag}_2\text{WO}_4$  (JCPDS Card: 34-0061,  $a=10.82$ ,  $b=12.01$ ,  $c=5.90\text{ \AA}$ ) as shown in Figure 7a. Anorthic  $\text{Ag}_2\text{W}_2\text{O}_7$  phase (JCPDS Card: 75-1506,  $a=6.033$ ,  $b=7.051$ ,  $c=7.735\text{ \AA}$ ,  $\alpha=73.8$ ,  $\beta=92.2$ ,  $\gamma=104.7^\circ$ ) was obtained at pH 2 (Figure 7b). TEM observation shows that both phases are in form of wire-like structures. A typical TEM image in Figure 7a indicated that  $\text{Ag}_2\text{W}_2\text{O}_7$  nanowires are uniform with diameter 50 nm and length up to micrometers. Electron diffraction pattern in Figure 8b taken along  $\langle 010 \rangle$  zone axis indicated that the nanowires are perfect single crystals. These nanowires can be doped into glass to produce conducting glass, which could give different conducting performances. Further work is still underway.

From the viewpoint of crystallography, the shape of the mesoscale or macroscale crystals is in fact the outside embodiment of the intrinsic cell structure. The high anisotropic growth we observed in molybdate systems could be related with the intrinsic crystal habit.<sup>[36]</sup> The promotion of anisotropic growth of nanorods/nanowires in ligand-free system could be related with several parameters, including the intrinsic structural features of specific faces, the local solution

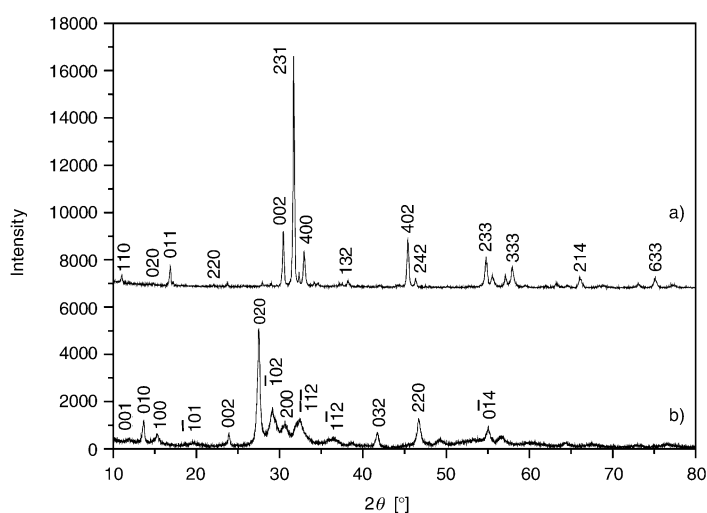


Figure 7. XRD pattern of  $\alpha\text{-Ag}_2\text{WO}_4$  nanorods and  $\text{Ag}_2\text{W}_2\text{O}_7$  nanowires synthesized at pH 9 and 2, respectively.

details, the foreign energy activation, and the autogenous pressure.<sup>[36]</sup> The detailed formation mechanism of such 1D nanostructures under hydrothermal conditions need more clarification in future.

About results demonstrate that it is possible to produce various molybdates and tungstates with different phase due

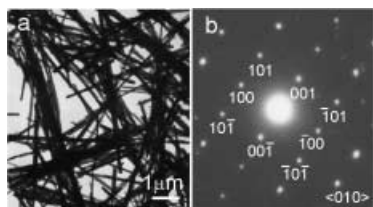


Figure 8. a) TEM image of  $\text{Ag}_2\text{W}_2\text{O}_7$  nanowires synthesized at  $140^\circ\text{C}$  for 12 h. b) Electron diffraction pattern taken along  $[010]$  zone axis.

to their rich families of polyanion species formed in the solution. Further understanding the solution chemistry of molybdates and tungstates will be very helpful for systematic synthesis of various kinds of nanowires/nanorods through this approach. Our elementary results show that other transition metal molybdate nanorods such as  $\text{NiMoO}_4$ ,  $\text{CuMoO}_4$ , and  $\text{PbMoO}_4$  could be synthesized through the similar method, indicating that the present approach could be a general approach for the synthesis of other rich family of metal molybdate nanorods/nanowires. These low dimensional materials could find important applications in various fields.

## Conclusion

In summary, we have shown that selective synthesis of uniform single crystalline silver molybdate/tungstate nanorods/nanowires in large scale can be realized by a facile hydrothermal re-crystallization technique. The synthesis is found to be strongly dependent on pH, temperature, and reaction time. Extremely long  $\text{Ag}_6\text{Mo}_{10}\text{O}_{33}$  single crystal nanowires covered with a lot of tiny nanoparticles can be obtained at pH 2. The pH dependent phase transition process was discussed. Similarly,  $\text{Ag}_2\text{WO}_4$ , and  $\text{Ag}_2\text{W}_2\text{O}_7$  nanorods/nanowires with diameter 50 nm and length up to micrometers can also be selectively synthesized by controlling pH value. The results demonstrated that it is possible to selectively synthesize other family of molybdate nanowires with controllable phases and structural specialty. The discovery of this new family of molybdate nanowires could lead to new applications of these materials. Further extension of this approach and investigation on their property of these new kinds of 1D nanobuilding blocks are ongoing.

## Experimental Section

Analytical grade  $\text{AgNO}_3$ ,  $(\text{NH}_4)_6\text{Mo}_7\text{O}_{24}$ ,  $\text{Na}_2\text{MoO}_4 \cdot 2\text{H}_2\text{O}$ , and  $\text{Na}_2\text{WO}_4 \cdot 2\text{H}_2\text{O}$  were purchased from Shanghai Chemical Industrial Company and were used without further purification. The reaction was carried out in a 60 mL capacity Teflon-lined stainless steel autoclave, which was done in a digital type temperature controlled oven.

In a typical procedure, 0.71 mmol analytical grade  $(\text{NH}_4)_6\text{Mo}_7\text{O}_{24}$  was dissolved in 30 mL distilled water and 5 mmol  $\text{AgNO}_3$  was dissolved in 20 mL distilled water, respectively. Then  $(\text{NH}_4)_6\text{Mo}_7\text{O}_{24}$  solution was slowly added into  $\text{AgNO}_3$  solution under magnetic stirring to form a homogeneous green-yellow solution at room temperature. The pH was adjusted to a specific value using  $\text{NaOH}$  or  $\text{HNO}_3$  ( $1 \text{ mol L}^{-1}$ ) solution. The

resulting precursor suspension was transferred into a Teflon-lined stainless autoclave. The autoclave was sealed and maintained at  $140^\circ\text{C}$  for 12 h, then allowed to cool to room temperature naturally. The green-yellow products were filtered off, washed several times with distilled water and absolute ethanol, and finally dried in a vacuum at  $60^\circ\text{C}$  for 4 h.

The products were characterized by X-ray diffraction pattern (XRD), recorded on a MAC Science Co. Ltd. MXP 8 AHF X-ray diffractometer with monochromatized  $\text{Cu}_{K\alpha}$  radiation ( $\lambda = 1.54056 \text{ \AA}$ ); transmission electron microscopy (TEM) and high-resolution transmission electron microscopy (HRTEM), performed on a Hitachi (Tokyo, Japan) H-800 transmission electron microscope (TEM) at an accelerating voltage of 200 kV, and a JEOL-2010 high-resolution transmission electron microscopy (HRTEM), also at 200 kV, respectively. X-ray photoelectron spectra (XPS) were recorded on an ESCALABMKII instrument with  $\text{Mg}_{K\alpha}$  radiation as the exciting source. The binding energies obtained in the XPS analysis were corrected by referencing the C 1s line to 284.60 eV.

## Acknowledgement

S.H.Y. acknowledges the special funding support from the Century Program of the Chinese Academy of Sciences and the Natural Science Foundation of China (The Distinguished Young Fund and Project No. 50372065).

- [1] a) M. G. Bawendi, M. L. Steigerwald, L. E. Brus, *Annu. Rev. Phys. Chem.* **1990**, *41*, 477; b) A. P. Alivisatos, *Science* **1996**, *271*, 933; c) H. Weller, *Angew. Chem.* **1993**, *105*, 43; *Angew. Chem. Int. Ed.* **1993**, *32*, 41.
- [2] a) X. Duan, Y. Huang, Y. Cui, J. Wang, C. M. Lieber, *Nature* **2001**, *409*, 66; b) N. I. Kovtyukhova, T. E. Mallouk, *Chem. Eur. J.* **2002**, *8*, 4355.
- [3] a) C. M. Lieber, *Solid State Commun.* **1998**, *107*, 607; b) J. T. Hu, T. W. Odom, C. M. Lieber, *Acc. Chem. Res.* **1999**, *32*, 435.
- [4] a) T. S. Ahmadi, Z. L. Wang, T. C. Green, A. Henglein, M. A. El-Sayed, *Science* **1996**, *272*, 1924; b) J. S. Bradley, B. Tesche, W. Busser, M. Maase, M. T. Reetz, *J. Am. Chem. Soc.* **2000**, *122*, 4631.
- [5] a) X. G. Peng, L. Manna, W. D. Yang, J. Wickham, E. Scher, A. Kadavanich, A. P. Alivisatos, *Nature* **2000**, *404*, 59; b) Z. A. Peng, X. G. Peng, *J. Am. Chem. Soc.* **2001**, *123*, 1389; c) Z. A. Peng, X. G. Peng, *J. Am. Chem. Soc.* **2002**, *124*, 3343.
- [6] Y. Cui, Q. Q. Wei, H. K. Park, C. M. Lieber, *Science* **2001**, *293*, 1289.
- [7] a) P. D. Yang, Y. Y. Wu, R. Fan, *Int. J. Nanotechnol.* **2002**, *1*, 1; b) G. R. Patzke, F. Krumeich, R. Nesper, *Angew. Chem.* **2002**, *114*, 2554; *Angew. Chem. Int. Ed.* **2002**, *41*, 2447.
- [8] a) H. Dai, E. W. Wong, Y. Z. Lu, S. Fan, C. Lieber, *Nature* **1995**, *375*, 769; b) W. Q. Han, S. S. Fan, Q. Q. Li, Y. D. Hu, *Science* **1997**, *277*, 1287.
- [9] a) J. D. Klein, R. D. Herrick, D. Palmer, M. J. Sailor, C. J. Brumlik, C. R. Martin, *Chem. Mater.* **1993**, *5*, 902; b) C. R. Martin, *Science* **1994**, *266*, 1961.
- [10] a) A. M. Morales, C. M. Lieber, *Science* **1998**, *279*, 208; b) M. Huang, S. Mao, H. Feick, H. Yan, Y. Wu, H. Kind, E. Weber, R. Russo, P. Yang, *Science* **2001**, *292*, 189; c) X. F. Duan, C. M. Lieber, *Adv. Mater.* **2000**, *12*, 298.
- [11] a) Z. W. Pan, Z. R. Dai, Z. L. Wang, *Science* **2001**, *291*, 1947; b) Z. R. Dai, Z. W. Pan, Z. L. Wang, *J. Am. Chem. Soc.* **2002**, *124*, 8673; c) J. Y. Lao, J. G. Wen, Z. F. Ren, *Nano Lett.* **2002**, *2*, 1287; d) J. Y. Lao, J. Y. Huang, D. Z. Wang, Z. F. Ren, *Nano Lett.* **2003**, *3*, 235; e) P. Yang, C. M. Lieber, *Science* **1996**, *273*, 1836.
- [12] W. E. Buhro, K. M. Hickman, T. J. Trentler, *Adv. Mater.* **1996**, *8*, 685.
- [13] J. D. Holmes, K. P. Johnston, R. C. Doty, B. A. Korgel, *Science* **2000**, *287*, 1471.
- [14] a) M. Li, H. Schnablegger, S. Mann, *Nature* **1999**, *402*, 393; b) C. N. N. Rao, A. Govindaraj, F. L. Deepak, N. A. Gunari, *Appl. Phys. Lett.* **2001**, *78*, 1853; c) N. R. Jana, L. Gearheart, C. J. Murphy,

- Adv. Mater.* **2001**, *13*, 1389; d) S. Kwan, F. Kim, J. Akana, P. Yang, *Chem. Commun.* **2001**, 447.
- [15] S. H. Yu, M. Antonietti, H. Cölfen, M. Giersig, *Angew. Chem.* **2002**, *114*, 2462; *Angew. Chem. Int. Ed.* **2002**, *41*, 2356.
- [16] a) R. L. Penn, J. F. Banfield, *Science* **1998**, *281*, 969; b) C. Pacholski, A. Kornowski, H. Weller, *Angew. Chem.* **2002**, *114*, 1234; *Angew. Chem. Int. Ed.* **2002**, *41*, 1188.
- [17] Z. Y. Tang, N. A. Kotov, M. Giersig, *Science* **2002**, *297*, 237.
- [18] a) S. H. Yu, *J. Ceram. Soc. Jpn.* **2001**, *109*, S65; b) S. H. Yu, J. Yang, Z. H. Han, Y. Zhou, R. Y. Yang, Y. Xie, Y. T. Qian, Y. H. Zhang, *J. Mater. Chem.* **1999**, *9*, 1283; c) S. H. Yu, L. Shu, J. Yang, Z. H. Han, Y. T. Qian, Y. H. Zhang, *J. Mater. Res.* **1999**, *14*, 4157.
- [19] J. Yang, C. Xue, S. H. Yu, J. H. Zeng, Y. T. Qian, *Angew. Chem.* **2002**, *114*, 4891; *Angew. Chem. Int. Ed.* **2002**, *41*, 4697.
- [20] X. Wang, Y. D. Li, *Angew. Chem.* **2002**, *114*, 4984; *Angew. Chem. Int. Ed.* **2002**, *41*, 4790.
- [21] H. Liao, Y. Wang, X. Liu, Y. Li, Y. Qian, *Chem. Mater.* **2000**, *12*, 2819.
- [22] X. W. Lou, H. C. Zeng, *Chem. Mater.* **2002**, *14*, 4781.
- [23] B. L. Chamberland, J. A. Kafalas, J. B. Goodenough, *Inorg. Chem.* **1977**, *16*, 44.
- [24] a) T. Qi, K. Takagi, J. Fukazawa, *Appl. Phys. Lett.* **1980**, *36*, 278; b) P. Kozma, R. Bajgar, J. P. Kozma, *Radiat. Phys. Chem.* **2002**, *34*, 127.
- [25] L. G. Van Uitert, S. Preziosi, *J. Appl. Phys.* **1962**, *33*, 2908.
- [26] a) J. G. Rushbrooke, R. E. Ansorge, *Nucl. Instrum. Methods Phys. Res. A* **1989**, *280*, 83; b) H. Wang, F. D. Medina, Y. D. Zhou, Q. N. Zhang, *Phys. Rev. Sect. B* **1992**, *45*, 10356.
- [27] a) H. Grassmann, H. G. Moser, E. Lorenz, *J. Lumin.* **1985**, *16*, 109; b) K. Tanaka, T. Miyajima, N. Shirai, Q. Zhang, R. Nakata, *J. Appl. Phys.* **1995**, *77*, 6581; c) H. Wang, F. D. Medina, D. D. Liu, Y. D. Zhou, *J. Phys. Condens. Matter* **1994**, *6*, 5373.
- [28] W. Qu, W. Wlodarski, J.-U. Meyer, *Sens. Actuators B* **2000**, *64*, 76.
- [29] E. Ehrenberg, H. Weitzely, C. Heidy, H. Fuessy, G. Wltschekz, T. Kroenerx, J. van Tol, M. Bonnet, *J. Phys. Condens. Matter* **1997**, *9*, 3189.
- [30] a) A. W. Sleight, *Acta Crystallogr. Sect. B* **1972**, *28*, 2899; b) S. Driscoll, U. S. Ozkan, *Stud. Surf. Sci. Catal.* **1994**, *82*, 367.
- [31] H. E. Swanson, M. C. Morris, R. P. Stinchfield, E. H. Evans, *NBS Monogr. (US)* **1963**, *25*, 24.
- [32] M. Bonanni, L. Spanhel, M. Lerch, E. Füglein, G. Müller, F. Jermana, *Chem. Mater.* **1998**, *10*, 304.
- [33] a) A. M. Beale, G. Sankar, *Chem. Mater.* **2003**, *15*, 146; b) A. Sen, P. Pramanik, *Mater. Lett.* **2002**, *52*, 140.
- [34] E. J. Wenda *J. Therm. Anal. Calorim.* **1998**, *53*, 861.
- [35] a) A. K. Arof, K. C. Seman, A. N. Hashim, R. Yahyar, R. Ahya, M. J. Maah, S. Radhakrishna, *Mater. Sci. Eng. B* **1995**, *31*, 249; b) K. Hariharan, C. Sangamithra, *Mater. Chem. Phys.* **1992**, *32*, 240.
- [36] S. H. Yu, B. Liu, M. S. Mo, J. H. Huang, X. M. Liu, Y. T. Qian, *Adv. Funct. Mater.* **2003**, *13*, 639.
- [37] a) X. Bao, M. Muhler, T. Schedel-Niedrig, R. Schlögl, *Phys. Rev. B* **1996**, *54*, 2249; b) S. W. Gaarenstroom, N. Winograd, *J. Chem. Phys.* **1977**, *67*, 3500.
- [38] S. Günther, M. Marsi, A. Kolmakov, M. Kiskinova, M. Noeske, E. Taglauer, G. Mestl, U. A. Schubert, H. Knözinger, *J. Phys. Chem. B* **1997**, *101*, 10004.
- [39] E. M. Tejada-Rosales, J. Rodriguez-Carvajal, N. Casan-Pastor, P. Alemany, E. Ruiz, M. S. El-Fallah, S. Alvarez, P. Gomez-Romero, *Inorg. Chem.* **2002**, *41*, 6604.

Received: August 5, 2003 [F5429]